Cerebral Cortex, 2023, 1–14
https://doi.org/10.1093/cercor/bhad440
Original Article

Motor cortex activation during visuomotor transformations: evoked potentials during overt and imagined movements

Nikolay Syrov[1,*], Lev Yakovlev[1], Alexander Kaplan[1,2], Mikhail Lebedev[3]

[1]Vladimir Zelman Center for Neurobiology and Brain Rehabilitation, Skolkovo Institute of Science and Technology, Bolshoy Boulevard 30, bld. 1. Moscow, 121205, Russia,
[2]Faculty of Biology, Lomonosov Moscow State University, 1-12 Leninskie Gory, Moscow, 119991, Russia,
[3]Faculty of Mechanics and Mathematics, Lomonosov Moscow State University, 1 Leninskiye Gory, Moscow, 119991, Russia

*Corresponding author: Email: kolascoco@gmail.com

Despite the prevalence of visuomotor transformations in our motor skills, their mechanisms remain incompletely understood, especially when imagery actions are considered such as mentally picking up a cup or pressing a button. Here, we used a stimulus–response task to directly compare the visuomotor transformation underlying overt and imagined button presses. Electroencephalographic activity was recorded while participants responded to highlights of the target button while ignoring the second, non-target button. Movement-related potentials (MRPs) and event-related desynchronization occurred for both overt movements and motor imagery (MI), with responses present even for non-target stimuli. Consistent with the activity accumulation model where visual stimuli are evaluated and transformed into the eventual motor response, the timing of MRPs matched the response time on individual trials. Activity-accumulation patterns were observed for MI, as well. Yet, unlike overt movements, MI-related MRPs were not lateralized, which appears to be a neural marker for the distinction between generating a mental image and transforming it into an overt action. Top-down response strategies governing this hemispheric specificity should be accounted for in future research on MI, including basic studies and medical practice.

Key words: stimulus–response mapping; LRP; motor imagery; reaction time; evidence accumulation.

Introduction

The majority of our movements are performed in the visual world, where complex visuomotor transformations enable motor precision (Jeannerod 1986). The visuomotor transformations are temporarily organized as stages of motor processing, including motor preparation, stimulus processing, motor execution (ME), and feedback (Bernstein 1947; Rahman et al. 2019). Movement-related cortical potentials (MRPs) are reflective of these stages with high temporal resolution (Vaughan Jr. 1969; Berchicci et al. 2016). Conventionally, MRPs are divided into 2 distinct components. The first component is a lateralized rapid negative deflection, which represents a movement-specific electrical potential that appears ~200–60 ms prior to movement onset. This potential has a contralateral negativity and is often described as the lateralized readiness potential (LRP), which is defined as the difference in electrical activity between the 2 hemispheres (Deecke et al. 1976; Trevena and Miller 2002; Neafsey 2021). The second MRP component is the reafferent potential (RAP) that occurs after movement onset. The RAP is characterized by a contralateral positive peak (Vaughan Jr. 1969; Syrov et al. 2022). Movement-related afferent signals (kinesthetic, tactile and visual) contribute to RAP formation (Bötzel et al. 1997; Berchicci et al. 2016).

Stages of motor processing also occur during motor imagery (MI), where individuals generate mental representations of movements, including imagining their associated sensations (Pfurtscheller 2000; Grush 2004; Stinear et al. 2006; Guillot et al. 2009). Neuroimaging and neurostimulation studies have consistently documented the similarity of cortical activity patterns during the overt and imagined movements, which both activate the primary motor cortex (M1) (Schnitzler et al. 1997; Fadiga et al. 1998; Grosprêtre et al. 2016; Mehler et al. 2019). Even though several studies pointed to the differences in cortical activity in these 2 cases (Caldara et al. 2004; Gabbard et al. 2009; Rodriguez et al. 2009; Glover et al. 2020; Yashin et al. 2023), there is still no clear explanation for the distinction between M1 activity that results in an overt action and the one that does not. However, knowledge of these mechanisms is important for understanding how movements can only be imagined and how this knowledge can be used in motor rehabilitation practice (Binkofski et al. 2002; Stippich et al. 2002; Jennings and van der Molen 2005). Thus, for the case of imagined visuomotor transformation, one could assume that visual information is propagated to motor cortical areas, but response initiation is blocked at some point and the mental effort does not end with actual muscle activation.

Multiple covert factors could motivate movements and influence the conversion of sensory information into motor preparatory activity (Jennings and van der Molen 2005), and thus contribute to LRP formation (Van Vugt et al. 2014; Gherman et al. 2023). Indeed, the LRP can be described as an intermediate stage in the transformation of a stimulus into a motor response, with the early part being more sensory and the late part more motor (Hackley and Valle-Inclan 1998; Gherman et al. 2023).

For the case of MI, Marc Jeannerod proposed a motor simulation theory, according to which covert and overt movements share the

Received: June 9, 2023. **Revised:** October 24, 2023. **Accepted:** October 25, 2023

neural substrates (Jeannerod 1994; Jeannerod 2001; Glover and Dixon 2013). Yet, the accumulation of motor activity during MI is not sufficient to trigger an actual execution. Consistent with this theory, Galdo et al. (2016) reported that LRPs were weaker during MI than during overt actions. In contrast, Hohlefeld et al. (2011) reported the absence of any lateralization in MI-related components. Thus, LRP characteristics specific to MI remain unclear. In particular, it is unclear whether movement suppression which is required for MI causes a decrease in LRP amplitude or a shortening of its duration. The latter effect could occur because the accumulation of activity preceding the imagined response is suppressed to prevent the activity from crossing the execution threshold. Alternatively, the preparation of an imagined response could involve a completely different cortical network as compared with the circuitry involved in the preparation of an overt action.

In addition to MRPs, electroencephalographic (EEG) spectral power is modulated during motor preparation and execution, particularly in the μ (7–15 Hz) and β (15–30 Hz) frequency bands, where event-related desynchronization (ERD) develops (Pfurtscheller et al. 2003). β-band ERD can occur as early as 2 s before movement (Pfurtscheller et al. 1997) and reflects premotor/motor activation. Movement-related sensorimotor ERD is temporally linked to motor execution process and processing of sensory reafference. However, ERD can also occur during MI in the absence of movements and their related reafferent inputs (Pfurtscheller 2000). In this context, MI can be conceptualized as a process of recalling or emulating how a movement feels (Grush 2004). Since a motor image incorporates somatosensory sensations, its retrieval leads to the activation of both motor and somatosensory areas (Savaki and Raos 2019).

Given these considerations, it is reasonable to suggest that preparatory processes involved in MI differ from the preparation of actual movements (Hohlefeld et al. 2011; Yashin et al. 2023). This difference in strategy could be reflected by LRPs and RAPs, and subsequently by their associations with the changes in oscillatory activity observed for real versus imagined responses. While associations between LRPs and μ−/β-ERD have been previously studied for both MI and ME (Fairhall et al. 2007; Ko et al. 2015; Galdo et al. 2016; Rogge et al. 2022), we did not find any studies that directly examined the relationship between RAP and movement-induced ERD, although RAP and μ-/β-ERD are thought to be related to afference processing. Notably, motor simulation theory, which could be used as a framework for understanding differences in MI and ME, has faced criticism, with several studies questioning its validity (Rodriguez et al. 2009; Gabbard et al. 2009; O'Shea and Moran 2017; Glover et al. 2020), which highlights the importance of studies comparing MRPs and spectral changes. To improve our knowledge of these issues, here we used a stimulus–response task to directly compare visuomotor transformation for both real and imagined movements. We analyzed the LRPs and their relationship to reaction time (RT) to investigate how the accumulation of stimulus-driven activity during the visuomotor transformation contributes to the properties of the LRP in real actions. A similar analysis was performed for the MI condition where we performed a procedure of epochs sorting based on the estimation of the response-related peak latency determined for each target trial. With these analyses, we assessed the temporal patterns of cortical activity during MI and ME. The study employed a block design to avoid different response strategies being intermixed. With this approach, we expected to find differences in the lateralization of MRPs preceding real versus imagined movements. Additionally, we analyzed the dynamics of the μ-/β-ERD with an expectation to find a correlation between RAP peaks and modulations of cortical oscillatory activity.

Methods

Participants

A total of 17 healthy volunteers with no history of neurological disorders and normal or corrected-to-normal vision (mean age 23 years, SD = 4; 6 female) participated in the study. All were right-handed according to the self-reports (no specific tests were performed to assess hand dominance). Participants had approximately 8 h of sleep, no alcohol or medication intake prior to the experimental session, and no coffee intake during the 2-h period preceding the experiments. All were informed of their rights and gave informed consent to participate in the study. The experimental procedures were approved by the Bioethics Committee of the Lomonosov Moscow State University (protocol no. 111-ch). The study followed the Declaration of Helsinki ethical principles for medical research involving human subjects. All subjects were informed of the study procedures and gave written consent to participate.

Experimental design

The subjects were seated at a table in a comfortable chair with their hands resting on a panel with 2 buttons (5 cm in diameter and 10 cm in height). The right and left buttons were dedicated for the right and left hand actions, respectively. During the experimental sessions, the buttons were highlighted using built-in LEDs in a semi-random sequence. The participants were instructed to pay attention only to the highlights of the button designated as the target and press that button as quickly as possible in the ME task or imagine performing a button press in the MI task. Mental counting (MC) of the target stimuli was used as a control condition, different from the other conditions in which a visuomotor transformation had to be presented. Since MI has no overt motor output (e.g. muscle activation), it was necessary to control the presence of sensorimotor activation in this condition. A block design was used, with each task being performed in a separate run (see Fig. 1). The order of runs was randomized across participants. Each run consisted of 6 consecutive sequences of trials (3 for each hand) and started with the presentation of the instruction word ("right" or "left") instructing the target button. The instructions were presented for 5 s on a 22-in LCD monitor placed in front of the subject. The target button (left or right) was randomly assigned for each sequence of trials. The stimulus sequence within each run consisted of 30 trials, each of 1,000 ms long: 200-ms button highlight followed by 800-ms interstimulus interval (ISI). Highlights of the target button required an action (ME, MI, or MC) to be performed, whereas non-target stimuli had to be ignored. Target and non-target stimuli were equal in numbers ($n = 15$ for each stimuli per trial) and randomly intermixed. These settings resulted in 90 target (45 right + 45 left) and 90 non-target responses collected for each task in a given participant. The experimental design is graphically illustrated in Fig. 1.

Signal acquisition

EEG was recorded at 1,000 Hz using an NVX-52 DC amplifier (MKS, Russia) with 22 Ag/AgCl passive electrodes in the following positions: *Fp1, Fp2, Fz, FC3, FCz, FC4, C5, C3, Cz, C4, C6, CP3, CPz, CP4, P3, Pz, P4, PO3, POz, PO4, O1, O2 (with correspondence to the international 10/10 system)*. Fp1 and Fp1 channels served as EOG-channels to remove eyes-blinking artifacts. The average of channels A1 and A2 was used as the reference. The electrode–skin impedance

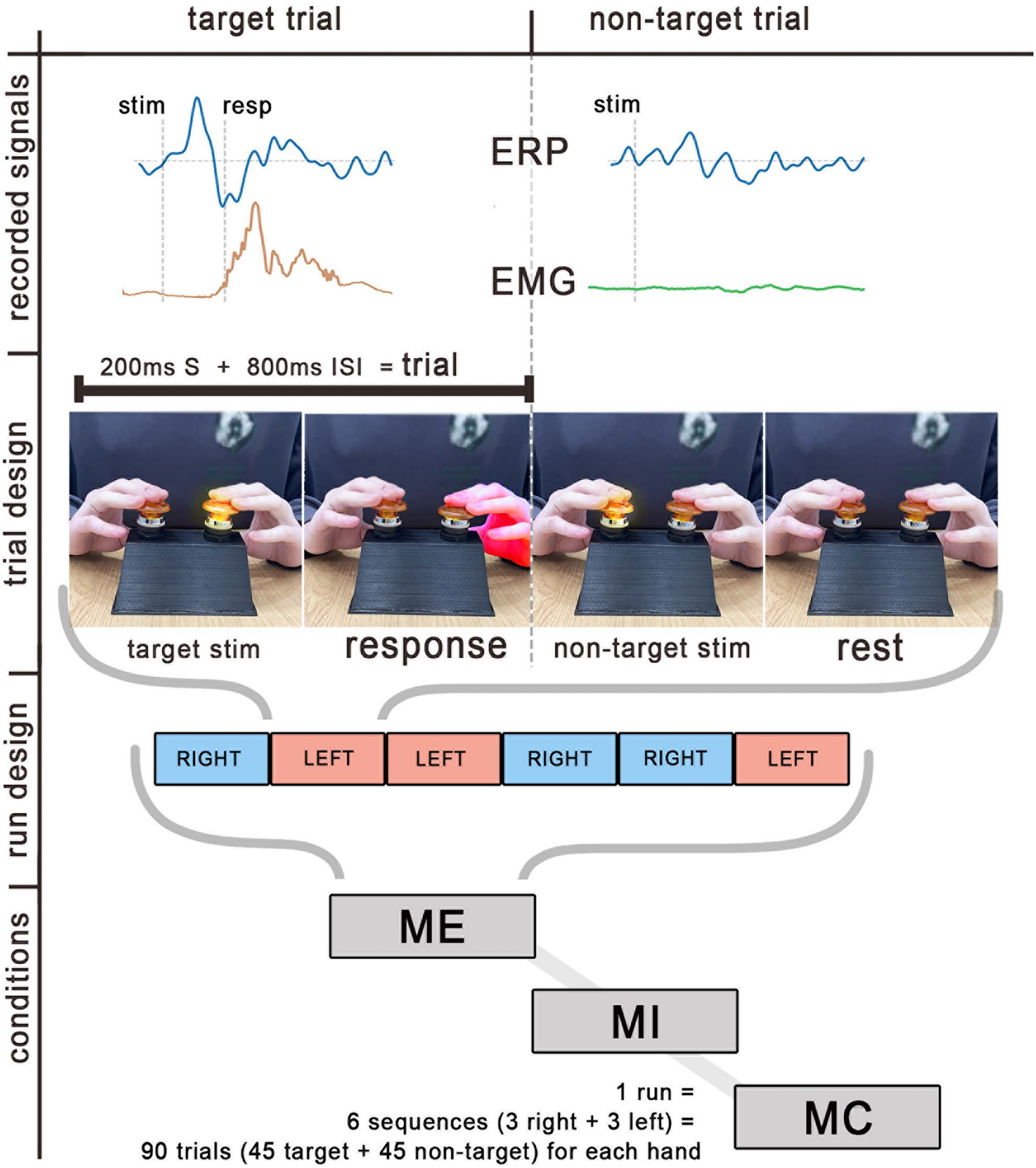

Fig. 1. Experimental design. Within each experimental session, 3 conditions were used: ME, MI, and MC. There were a total of 3 runs (1 run per condition) consisting of 6 sequences of trials (3 for each hand). Each sequence of trials started with a command indicating which button was the target (right or left). Participants focused on the target button highlights to which they responded by pressing the target button, imagery of button press, or counting the number of highlights for the ME, MI, and MC tasks, respectively. Each sequence contains 30 trials of button highlights, which were target and non-target highlights in equal proportion (15 + 15). The total number of trials per run for each hand was $n = 90$ (45 target + 45 nontarget). The flash duration was 200 ms (S) and the ISI was 800 ms. EEG and EMG signals were recorded. Stimulus presentation time and response time were synchronized with the signal recording. EEG and EMG signal epochs recorded during target and non-target trials are shown at the top of the figure.

was kept below 20 kΩ. The stimulus presentation time and the button press timestamps were synched with signal acquisition. Two channels of surface EMG for the left-hand and right-hand *m. flexor digitorum superficialis* (FDS) were sampled in order to discard non-ME-trials and non-target trials where muscles were activated.

Event-related potentials analysis

The raw EEG signal was bandpass filtered using a Butterworth fourth-order filter with a frequency range of 1–15 Hz. Blinking artifacts were removed using independent component analysis (fastICA method). The components highly correlated with signals from Fp1 and Fp2 channels were classified as electrooculography-artifacts and then excluded from the signal. The preprocessed signal was epoched [−0.5–1] s after the visual stimulus onset; the mean voltage of the [−0.5–0] s period was used for the baseline correction. These “preprocessed epochs” were used in further analysis. Then the stimulus-locked averaging was used to compute target and non-target ERPs in each condition. Furthermore, to compare stimulus- and response-locked ERPs during the ME condition, averaging was performed for the data aligned on the button press. To visually compare the stimulus and response-aligned ERPs, the 298-ms shift was performed, which corresponded to accounting for the median RT calculated for all subjects.

To compute lateralized potentials across all experimental conditions, stimulus-locked epochs (as opposed to response-locked) were considered due to the lack of overt responses during the MI and MC tasks. Considering the contralateral predominance of both pre- and post-movement potentials, calculation of lateralized potentials (i.e. cortical potentials comprising pre-movement LRP and post-movement lateralized peak derived from the RAP) was performed using the double subtraction method introduced by Coles (1989) for LRP calculation (see Eq. 1). With this method, lateralized potentials were first computed separately for each trial by subtracting the ipsilateral potentials from the contralateral ones (C3 vs C4, see Eq. 1, *a* and *b*), followed by the averaging (Eq. 1, *c*):

$$\begin{aligned} &\mathrm{LRP_{right}} = \mathrm{C3_{ERP}} - \mathrm{C4_{ERP}} \quad &\text{a)} \\ &\mathrm{LRP_{left}} = \mathrm{C4_{ERP}} - \mathrm{C3_{ERP}} \quad &\text{b)} \\ &\mathrm{LRP} = \frac{\mathrm{LRP_{rigt}} + \mathrm{LRP_{left}}}{2} \quad &\text{c)} \end{aligned} \qquad (1)$$

Analysis of movement-related potentials

To analyze the relationship between the RTs and the preparatory and post-movement cortical potentials, single-trial lateralized responses were obtained from the ME data separately for each button press, that is, without averaging across trials (Eq. 1, *a*-*b*). The same approach was used by Falkenstein et al. (2006). The epochs with extra slow responses (with the RT exceeding the threshold of 577 ms calculated as $Q3 + 1.5IQR$ for the RT data) were discarded (2–3 epochs for each subject). All participants’ single-trial lateralized potentials were collected in 1 matrix and sorted by motor-response latency in ascending order. For better visualization, we applied a moving average with a 10-ms window and 1 timestamp step to each epoch, which produced smooth traces (Fig. 3A).

Amplitude, latency, and length of the LRPs were calculated. LRP amplitude was measured as the peak negative deflection within the time interval from the visual stimulus onset till 80 ms after the response. LRP’s latency was defined as the time of the peak value. The length of the LRP was determined for each trial by measuring the duration where the LRP absolute value exceeded half of the peak amplitude. Additionally, we measured the latency of the post-movement lateralized peak derived from RAP. The relations between these characteristics of the cortical potentials and the RT were quantified using a linear mixed model analysis.

To examine the presence of lateralized potentials for the non-target trials, we removed from the analysis all non-target epochs where EMG responses were detected (0.12% of all non-target trials).

Analysis of MI-related ERPs

For MI trials, the late positive peak occurring after the negative potential was considered as response-related. Since response onset could not be measured explicitly for the MI trials, an alternative approach was implemented to analyze cortical potentials reflecting the onset of imagined movements. We performed a trial-by-trial sorting based on the latency of the response-related positive potential estimated as the time point at which it peaked. This procedure is often used for latency correction (Picton et al. 2000; Poli et al. 2010). Since accurate alignment can be affected by EEG fluctuations that introduce noise, we used a peak-picking approach proposed by Gratton et al. (1989), which consists of an application of a band-pass filter (0.5–2 Hz) followed by smoothing with a 20-ms window sliding window (see also Makeig and Onton 2011; Ganin and Kaplan 2022). Thus, the latency of the MI-related positive peak was determined for each smoothed potential by identifying its maximum value for the interval 400–800 ms relative to stimulus onset. All trials were then sorted by latency in ascending order (like the sorting of the ME trials by RT).

Time–frequency analysis

Following the preprocessing described above, a time–frequency analysis was performed to estimate the depression of sensorimotor rhythms during ME and MI trials. EEG signals were re-referenced to the common average reference (McFarland et al. 1997). The Morlet wavelet transform was used for the analysis of the time–frequency perturbations. We used a set of complex Morlet wavelets with variable number of cycles for different frequencies. The frequencies ranged from 5 to 25 Hz with a 1-Hz step, and the full-width at half-maximum (FWHM) was equal to 374 ms. The desynchronization value was calculated as the ratio of the signal power during the target epochs to the median of the signal power during the [0.5–1 s] time interval of non-target epochs. The non-target trials were used for comparison, as it was reasonable to assume that they would not contain any sensorimotor responses. The obtained ratio was converted to decibels (see Eq. 2). Negative and positive values corresponded to ERD and synchronization (ERD/S), respectively.

$$\mathrm{ERD/S,\,dB} = 10 * \log_{10}\frac{\mathrm{power_{target}}}{\mathrm{power_{non-target}}} \qquad (2)$$

Median values were then calculated across all epochs to obtain ERD values for each of the experimental conditions (MI, ME, and MC) for each subject. To analyze the spatial scalp distribution of ERD in the individual frequency bands, we calculated the median value within the time range [0.3–0.7] s. For each participant, the individual frequency band was determined as the ERD peak frequency in the μ-/β-range (7–15/15–25 Hz) ± 2 Hz. In cases where no pronounced peak was observed, an a priori range was used. The resulting value was also used in a correlation analysis where the association was assessed between the changes in sensorimotor rhythms and post-movement RAP peaks.

Statistics

The cluster-level statistical permutation test was used to determine whether the target and non-target lateralized potentials significantly differed from zero (i.e. significance of the lateralization). A permutation cluster-based test was performed with cluster-level corrections that accounted for multiple comparisons. Specifically, a null distribution was generated from 100,000 random sets of permutations. Statistical significance was determined by evaluating the proportion of the elements in the null distribution that exceeded the observed maximum cluster level. The F-threshold was automatically selected to correspond to a P-value of 0.01, which controlled for the Type I error rate.

Pearson's correlation test was used to assess the relationship between RAP amplitude and movement-related ERD magnitude. To explore the relationship between LRP characteristics and the RTs, we used a linear mixed model analysis with RT as dependent variable, LRP latency and length as predictor variables, and subject as a random effect. Thus, we accounted for the inter- and intrasubject variability by considering all trials instead of averaging within subjects (Guthrie et al. 2018).

Results

EEG responses to target stimuli differed from those to non-target stimuli for all conditions (Fig. 2A). They consisted of an early positive component followed by negativity spanning the interval 200–400 ms after stimulus onset. These early responses were followed by a late positive component for the ME and MI conditions. Interestingly, for the left-target trials, the positive deflection was the strongest for channel C4 for the interval 400–700 ms (in Fig. 2A). No such late positivity was observed for the MC trials as was evident from the analyses of the difference between the ERP curves (Fig. 2A, bottom section).

To test whether the late positive peak was response-related, we performed response-locked averaging for the ME trials. Prior to the averaging, we detected the outlying slow responses (see Methods) and removed them from the analysis as noisy (Poli et al. 2010). Response-locked averaging of the ME-related epochs confirmed the locking of this component to the motor response (Fig. 2B), supporting that this was an RAP.

The RAP peak and the preceding LRP were the strongest in the hemisphere contralateral to the acting limb. Since the LRP peak was the most prominent for the stimulus-locked averaging, this averaging approach was used to compute the topography maps.

Motor lateralized potentials in motor execution and the RT

Figure 3A shows the across-participant aggregated epochs from the ME trials processed with a subtraction procedure (C3 minus C4 for the rightward responses and vice versa for leftward responses) and ordered by RT increase in ascending order. Here, time zero corresponds to visual stimulus onset, and motor response onset is represented by a bold dashed line. Two lateralized MRPs components were clear. The first component was the negative component that corresponded to the LRP (shaded in blue). For each trial, this component started ∼200 ms after the stimulus presentation, lasted until response onset, and faded either simultaneously with or shortly after the motor response. Significant positive correlations were found between the RT and LRP peak latency (estimated coefficient = 0.57, $P < 0.001$, std. error = 0.04) and between the RT and LRP duration (estimated coefficient = 0.58, $P < 0.001$, std. error = 0.024). No correlations were found between the LRP amplitude and RT (see Fig. 3B). Furthermore, when we used latency and LRP duration together for modeling, we obtained a better fit (LRP duration: coefficient = 0.86, std. error = 0.02; LRP latency: coefficient = 0.72, std. error = 0.03, $P < 0.001$).

While the LRP onset was time-locked to the stimulus, its duration extended to the motor response. The positive deflection of the EEG potential that followed the LRP (see Fig. 3A) was clearly time-locked to the motor response onset. A significant correlation was found between the latency of post-movement lateralized peak and the RT (estimated coefficient = 0.72, $P < 0.001$, std. error = 0.014, see Fig. 3B).

Figure 4 shows the grand-averaged stimulus-locked lateralized response for the target (blue line) and non-target (gray line) ME trials. For both target and non-target trials, cluster-based permutation tests revealed a significant ($P < 0.001$ and $P < 0.01$ for target and non-target, respectively) difference from the zero-level. The temporal clusters coincided with the LRP latency range, which corresponded to the premovement period defined by EMG onset. A small negative deflection for the non-target trials had a lower amplitude compared with the target trials. This deflection returned to the baseline by the time the EMG response began to develop during the target trials.

Target-trial lateralized responses were characterized by a significant contralateral post-movement positive potential ($P < 0.01$), derived from RAP, that peaked when muscle activity reached the maximum. The potential returned to baseline when the button was released.

MI-related potentials

The analysis of MI condition showed a positive component for the target response, which spanned the 500–700 ms interval with respect to stimulus onset. This interval overlapped with the latency interval of the RAP component for the real movements. We refer to this component as the RAP-like potential because it was maximal over the sensorimotor areas (i.e. channel Cz). In contrast to movement-evoked responses, the RAP-like potential during MI did not have a hemispheric lateralization (see Fig. 5A). Additionally, the negative component preceding the RAP-like peak was also not lateralized during MI, regardless of the hand being imagined. Finally, no lateralized component was found for the MC trials.

Figure 5B shows cortical potentials during MI, with trials sorted by latency of the RAP-like peaks in ascending order. It can be seen that the latency of the early positive peak was locked to the visual stimulus, whereas the negative wave preceding the RAP-like potential started ∼250 ms after the stimulus and lasted until the response-related positivity (i.e. the RAP-like peak) whose latency ranged from 400 to 800 ms.

ERD for the ME and MI responses

The analysis of event-related perturbations revealed a temporally reliable depression only for the β-band. Short-lasting contralateral ERDs were observed during both real and imagined responses, but not for the MC task. Figure 6A shows the grand-averaged time-frequency dynamics for the right-MI and left-MI conditions; channels C3 and C4 are shown. The most pronounced ERD occurred in the 15–25 Hz range and peaked 500–600 ms after the visual stimulus onset. Figure 6B shows the median for β-ERD in all conditions.

The amplitude of the β-ERD within the time interval 0.3–0.7 s was used in the correlation analysis whose aim was to assess the relationship between the sensorimotor ERD and RAP. Figure 6C shows that the correlation was negative between the amplitude of β-ERD from C3 and C4 channels (for right- and left-hand responses, respectively) and the amplitude of the RAP-like peak (from Cz channel). Pearson's test showed a strong significant correlation for both the right ($R = -0.75$; $P = 0.0006$) and left ($R = -0.70$; $P = 0.0017$) hands. To investigate these associations for real movements, we computed RAP amplitude and β-ERD for the alignment on response. In contrast to the MI condition, the overt

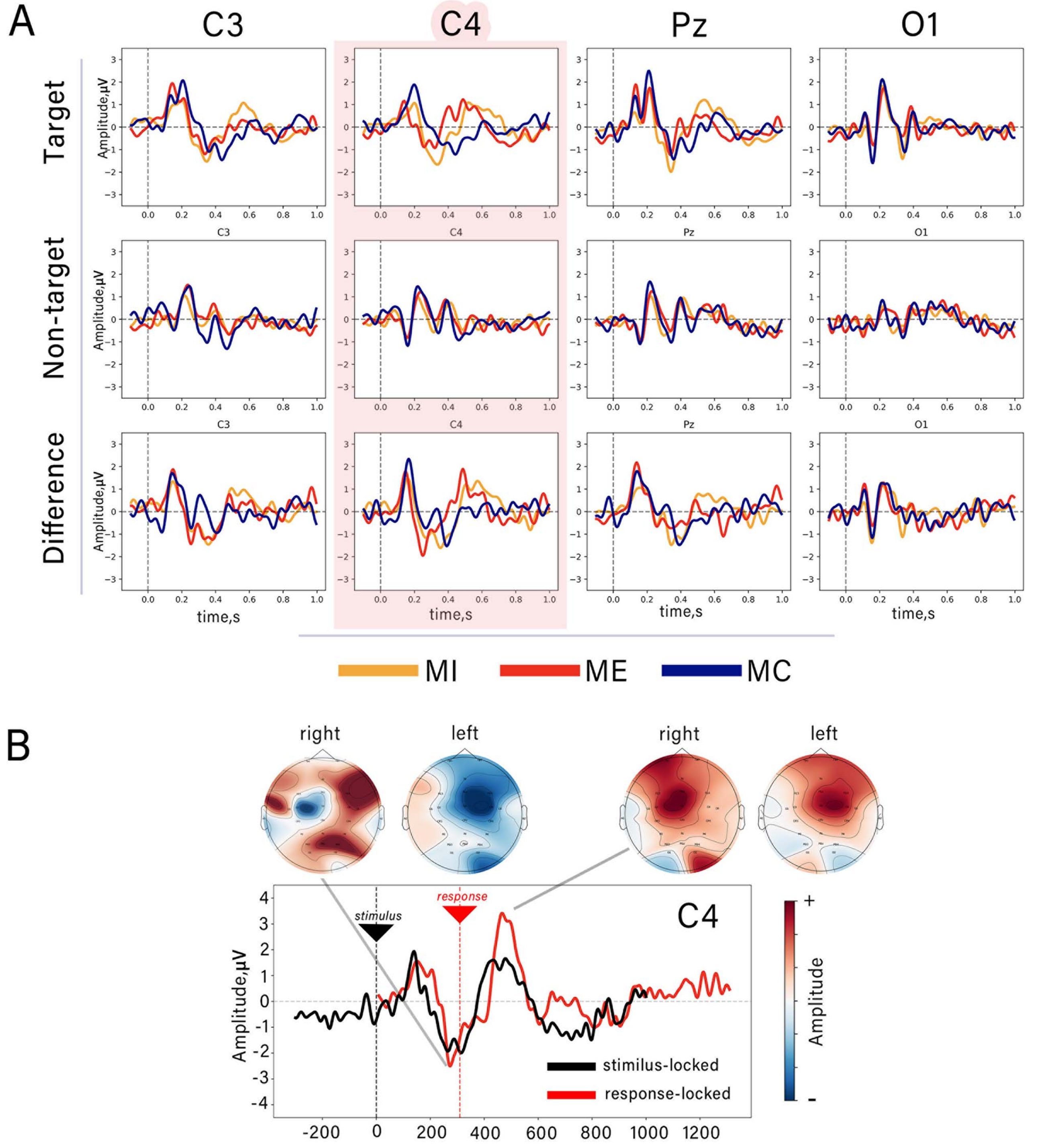

Fig. 2. (A) Group averaged ($n = 17$) stimulus-locked ERPs for targets and non-targets and their difference (target ERP minus non-target ERP) for the central, parietal, and occipital channels. Data are shown for MI, ME, and MC conditions for the trials in which the left button was assigned as the target. The ERPs from channel C4 are colored to highlight the data from the areas contralateral to the target. (B) Stimulus-locked (black solid line) and response-locked (red solid line) average MRPs (left-hand ME trials) for channel C4 plotted in the same graph. The plots also show the topographical distributions of the MRP peak amplitude. The distributions are shown separately for leftward and rightward responses.

movement condition had no relationship between ERD and RAP amplitude (see Fig. 6C).

Discussion

In this study, we investigated EEG responses to target and non-target visual stimuli for 3 response strategies: MC, overt button pressing (ME), and imagined button pressing (MI). Lateralized cortical potentials, indicative of limb-specific sensorimotor area activation, were assessed across these conditions. The primary goal of this analysis was to reveal the association between the lateralized potential parameters and specific response characteristics (response type and response latency). The analysis clarified the visuomotor transformation for the overt and imagined movements. In both cases, the visual stimulus elicited an activity over the sensorimotor cortex but only in the case of overt

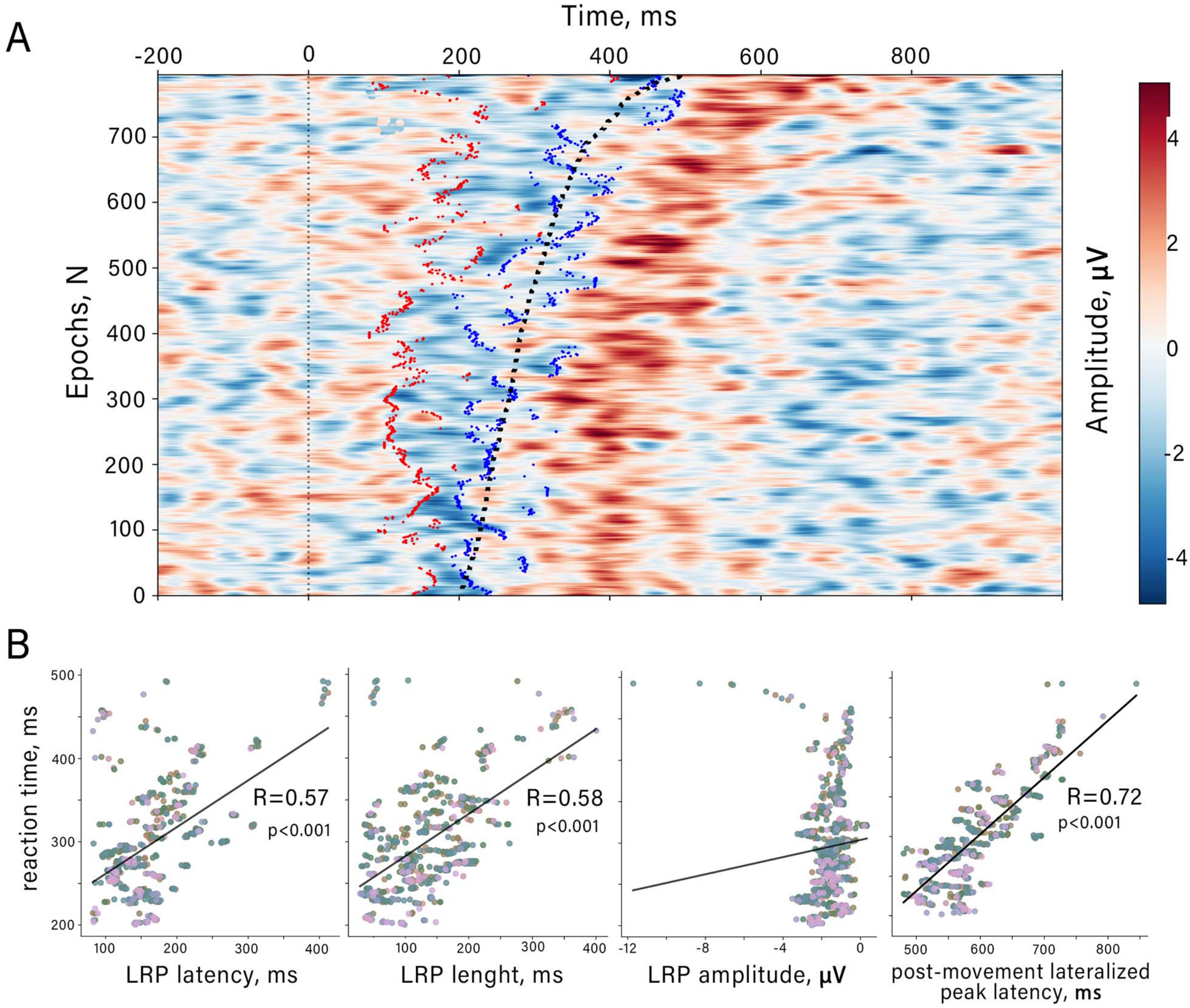

Fig. 3. (A) Lateralized potentials for all ME epochs in all participants sorted by RT (bold dashed line). The red and blue dots limit the LRP's onset and offset determined as the period where LRP deflection exceeded 50% of maximal amplitude. (B) Associations between response RT and lateralized potential parameters (from left to right: LRP's latency, LRP's length, LRP's amplitude, latency of post-movement lateralized peak derived from RAP. The color dots indicate different participants), estimated coefficients and *P*-values are presented in the graphs.

movements this activity culminated in an actual motor execution. Based on these results, we consider the hypothesis confirmed that LRP reflects a visuomotor transformation, where neural activity gradually accumulates within sensorimotor areas prior to motor execution. The theoretical framework of such an accumulation could be used to explain how accumulation unfolds even during the trials where no overt movements are executed. The role of response strategy in shaping LRPs is of particular interest.

The relationship between LRP characteristics and RT in terms of motor activity accumulation

Premovement LRPs with a pronounced lateralization were clear only in the ME trials. The amplitude was maximal over the frontocentral areas in the hemisphere contralateral to the active limb. Such an LRP develops in M1 prior to voluntary movements (typically about 200 ms prior the EMG onset), that is, during the period when a movement is being prepared (Böcker et al. 1994; Schmitz et al. 2019). This cortical potential has been suggested to reflect M1 preparatory activity during the ballistic stages of movements preparation (Logan and Cowan 1984; Schultze-Kraft et al. 2016) where at some point it becomes impossible to veto the upcoming movement (Schultze-Kraft et al. 2016; Neafsey et al. 2021). Yet, an LRP could reflect a more complex sensorimotor integration than just premovement effector-specific M1 excitation. Thus, LRP shape and latency depend on perceptual categorizing of the stimulus (e.g. linking the stimulus to the limb that has to move) and the subsequent action preparation and execution (Hackley and Valle-Inclan 1998). Luck et al. (2009) investigated LRP features representative of stimulus processing, and Saville et al. (2015) proposed that increased neural noise causes high variability LRP latency, and consequently RTs, in patients with attention deficit hyperactivity disorder. According to the drift-diffusion model, a stimulus being analyzed during decision making triggers a noisy evidence accumulation process in which the activity of neural circuits drifts toward a decision threshold (Van Vugt et al. 2014; Hanks et al. 2015). Based on this model, Van Vugt et al. (2014) proposed that the early part of the LRP reflects the accumulation of evidence, while the later phase is a self-maintaining ballistic stage formed by a motor network (Van Vugt et al. 2014).

Here, by examining the relationship between the single-trial lateralized EEG responses and the RTs, we clarified how LRPs

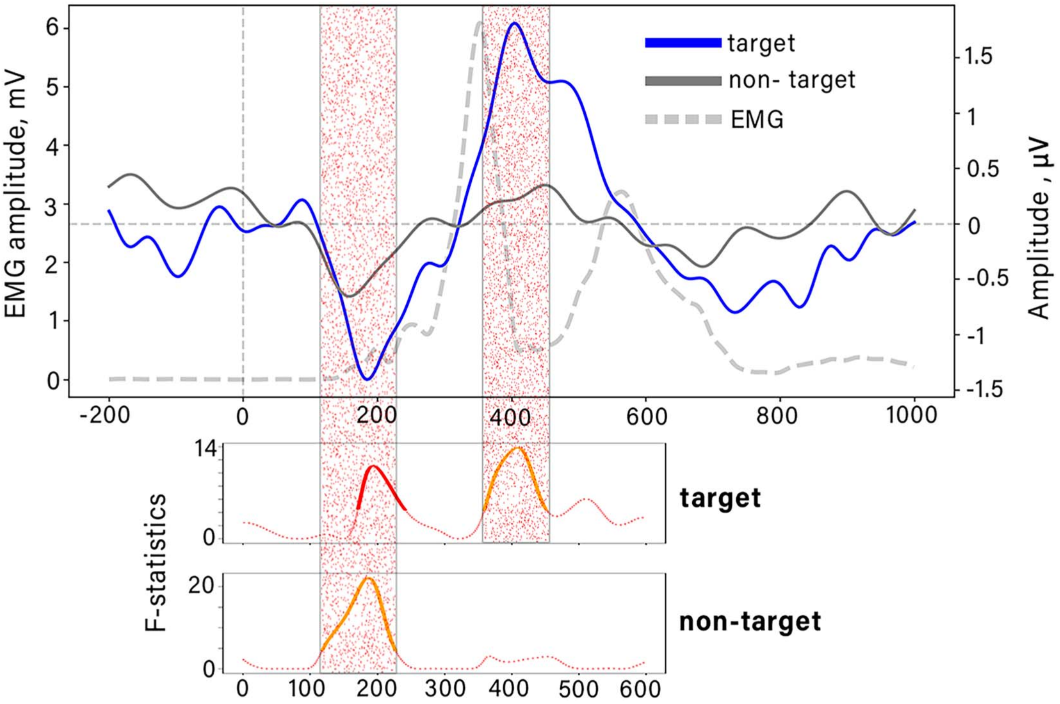

Fig. 4. (A) Stimulus-locked across-subject average lateralized potentials for target (blue line) and non-target (gray line) ME-trials. The dashed transparent gray line is an averaged EMG response corresponding to target trials. (B) Results of the nonparametric cluster-based permutation tests indicate the significant differences between lateralized response and zero. F-statistics is shown. For temporal cluster including target LRP p-value < 0.001, for two significant clusters including non-target LRP and post-movement positivity p-value < 0.01. Significant clusters are represented by bold lines, while the dotted line corresponds to insignificant differences.

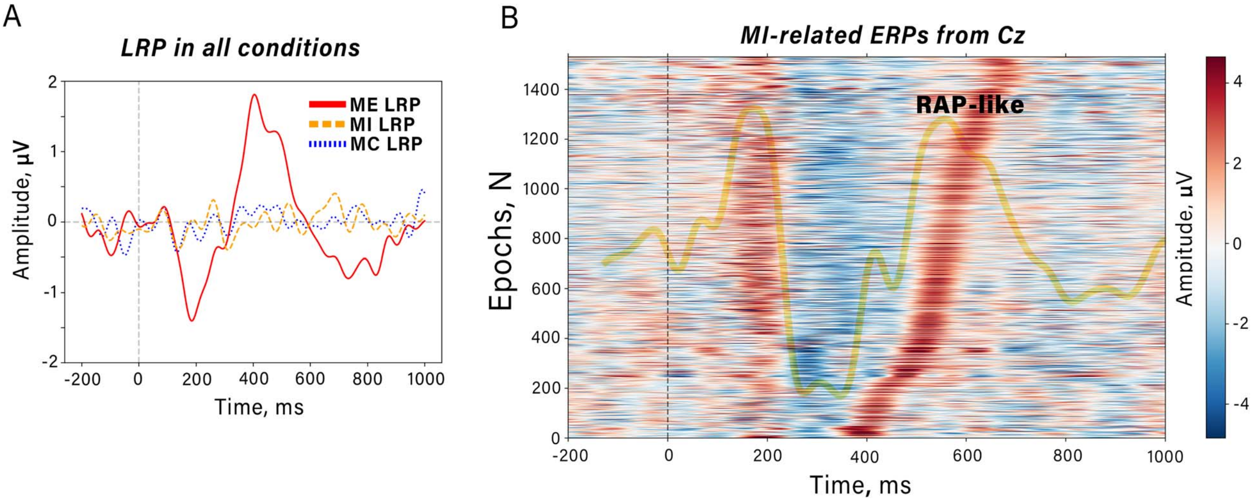

Fig. 5. (A) Lateralized potentials in 3 experimental conditions: MC, MI, and ME. (B) The epochs related to target MI-trials from Cz channel in all participants sorted by ascending of determined RAP-like latency time. The dashed line indicates stimulus onset. The grand averaged ($n=17$) MI-related ERP from the Cz channel is overlaid on the figure as a transparent line.

represent an activity accumulation process during a visuomotor transformation. We found a significant correlation between LRP timing and RT. Furthermore, we found a significant correlation between the response time and LRP length. These findings suggest that response delays are associated with a slower increase in excitability in motor cortical networks. Indeed, not only did the LRP shift synchronously with the RT, but its duration also increased with the increase in response timing. These results are consistent with the findings of Sangals et al. (2002) who described a shortening of LRPs for faster motor responses and Falkenstein et al. (2006) who reported an increase in LRP duration associated with RT slowing in the elderly population. At the same time, our results are hard to explain in terms of the suggestion of Van Vugt et al. (2014) who proposed that the late part of the LRP is the result of activation of a "threshold layer" of M1 neurons that are not involved in activity accumulation but only translate inputs into motor execution. Based on our results, LRP length, but not LRP peak amplitude, affects the RT, which is consistent with the model where the slope of increasing neural activity (rather than its peak amplitude) causes reaching a fixed threshold after which a response is elicited (Hanes and Schall 1996; Sangals et al. 2002). Our results agree with the recent findings of Li et al. (2023) who

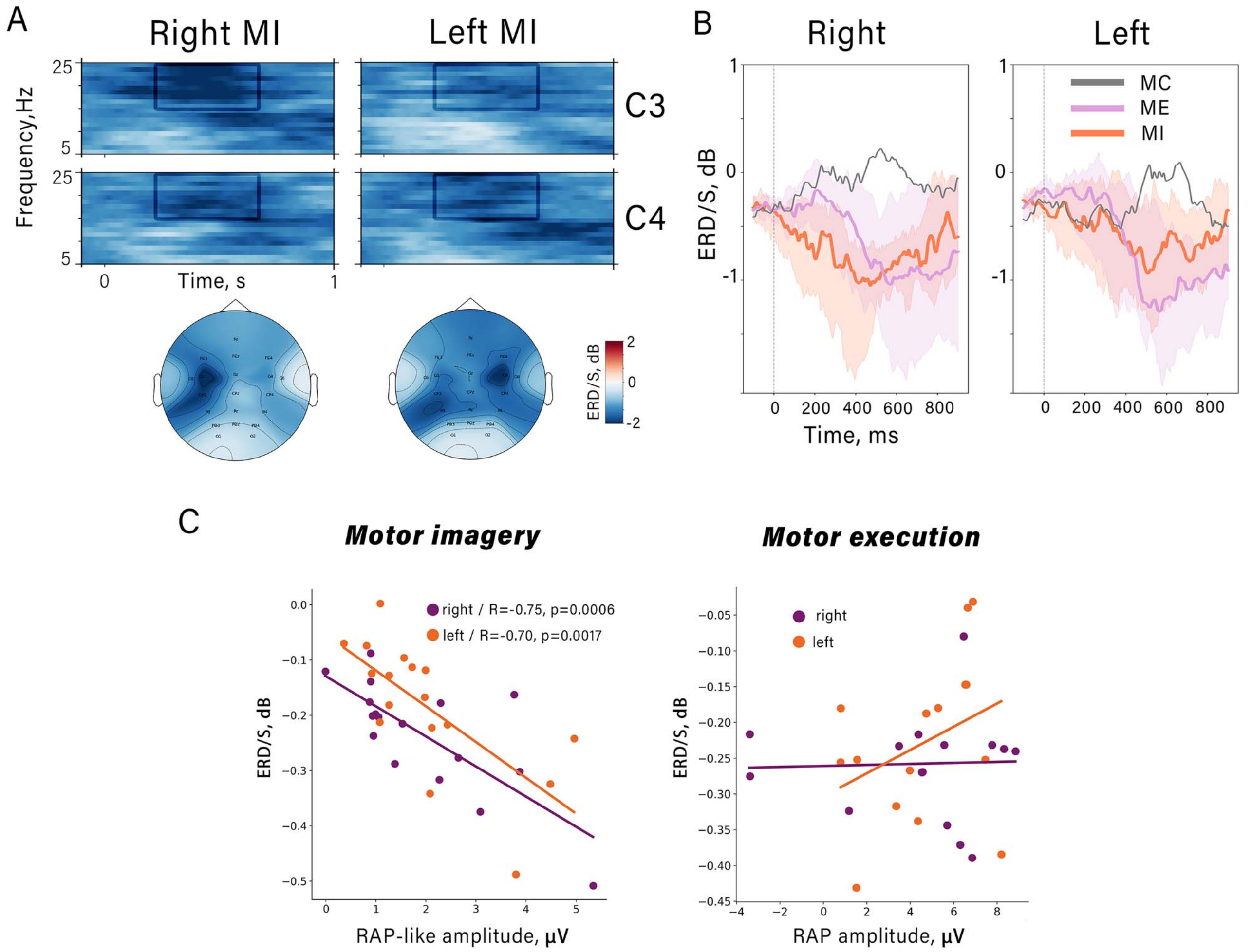

Fig. 6. (A) Across-subject ($n = 17$) median values showing the time–frequency dynamics for MI target trials for C3 and C4 channels and the corresponding topography distribution (bottom). The rectangles on time–frequency plots highlight the time [0.3–0.7] s and individual frequency (15–25 Hz) ranges used for β-ERD topography estimation. (B) Median time courses of β-ERD for all experimental conditions in C3 channel for right-responses and C4 for left-responses. The transparent shapes indicate the interquartile range. (C) Intersubject correlations between β-ERD value (time and frequency ranges were the same as described for Fig. 6A) and RAP-like/RAP peak amplitude for left and right MI/ME responses. RAP-like peak amplitude was calculated as the average value across the time interval ± 20 ms relative to the maximal positive deflection within the time window [0.5–0.7] s. Correlation coefficients and P-values are shown.

demonstrated an early stimulus-locked activation that persisted until the motor response in the parietal and precentral areas. Regarding the reason why some responses were slower than the others, we could speculate that fluctuations in M1 excitability could have played a role (Misirlisoy and Haggard 2014; Paluch et al. 2021; Aksiotis and Ossadtchi 2022) since M1 readiness to execute a movement is known to be influenced by internal factors (Kunzendorf et al. 2019; Al et al. 2021) and stochastic processes (Murakami et al. 2014; Murakami et al. 2017; Aflalo et al. 2022).

Non-target LRPs

In the examination of non-target LRPs, it was of interest to investigate the presence of lateralized activation in M1 during non-target ME trials, that is, the trials where no movements were produced but some kind of subthreshold movement preparation could have taken place. We expected that the use of a block design with the response strategy aimed at fast button press would facilitate such subthreshold activity even in response to non-target flashes. At the same time, we expected these LRPs to be weaker compared with target ME trials, since non-target trials should not lead to actual movements and the stimulus-driven accumulation of activity reflected in LRPs must be aborted.

Consistent with our expectation, even though participants in these experiments focused their attention on the target stimuli and ignored the distracting non-targets, LRPs were observed in response to non-targets. These non-target LRPs were weak and of shorter duration compared with the target responses (Fig. 4). Although target and non-target LRPs started at the same time relative to the stimulus, non-target LRPs returned to baseline at the time that matched EMG onset in the target trials. The presence of non-target LRPs agrees with the model of decision-making where sensory information is evaluated in the context of the instructed motor task and a veto decision results from this evaluation. The motor circuits could have been in a state of permanent readiness to react as quickly as possible, so that all visual stimuli initiated a visuomotor transformation process, where the ME was allowed to fully develop only in the target trials. Previously, Carrillo-de-la-Pena et al. (2006) observed double-peak LRPs. They suggested that the first peak could have represented the selection of the acting hand prior to the final decision on whether or not to initiate a movement. In a paradigm similar to our non-target trials, Galdo et al. (2016) showed that LRPs were weaker in no-go trials, where participants successfully stopped movement preparation. Conversely, LRPs were stronger in the no-go trials where the participants failed to stop movement. Thus, non-target LRPs indicate that cortical motor areas do not remain silent during stimulus evaluation, and the mere presence of an LRP does not necessitate an imminent motor response, nor does it necessitate the occurrence of action awareness.

An absence of lateralized potentials during MI

Although the lateralization of cortical potentials was very clear in the ME task, even in both target- and non-target we did not observe any lateralization during MI. This result is different from the findings of several previous reports where LRPs during MI resembled those during ME and were weaker in amplitude (Galdo et al. 2016) or even comparable (Caldara et al. 2004). Furthermore, an inversion of LRP polarity was observed when foot movements were imagined (Carrillo-de-la-Pena et al. 2006). Although these previous results appear to support high similarity of cortical potentials associated with the executed and imagined movements, our present findings show that this conclusion cannot be extended to all experimental conditions. Similar to our present results, Hohlefeld et al. (2011) did not find lateralization of cortical potentials for imagined and quasi-movements of the hand. They suggested that sensorimotor activation was weak in the absence of overt movements. Such weak activity without lateralization could correspond to response preparation preceding the selection of the acting limb (Saville et al. 2015). In support of this view, a conversion from non-lateralized to lateralized activity was demonstrated by Carrillo-de-la-Peña et al. (2008). They observed such a conversion for both ME and MI conditions in a paradigm where an imperative stimulus evoked a non-lateralized negativity that became lateralized after the presentation of a cue instructing which hand should act overtly or imaginarily.

It should be noted that we used a block design where subjects did not change the working hand in a block of trials, so there was no trial by trial requirement to select the type of motor response anew. These settings could explain the absence of lateralized cortical potentials in the MI condition because, as suggested by Carrillo-de-la-Peña et al. (2008), MI causes activation in the M1 similarly to actual execution during the working hand selection, but not during the other processing stages.

Despite the absence of lateralized responses, significant β-ERD occurred during MI trials but not during MC trials. β-ERD developed during ME trials, as well. Assuming that β-ERD is a sign of increased motor cortical activity (Yousry et al. 1997) it is reasonable to suggest that such activation reflects the presence of a sensorimotor activation in both ME and MI conditions. Our observations of the differences in the LRPs in the presence of β-ERD in the MI and ME conditions are consistent with the previous report by Hohlefeld et al. (2011). This suggests that although there were similarities between these 2 conditions, as predicted by simulation theory (Jeannerod 2001), imagining actions and executing them were enabled by separate states of cortical motor circuits. Specifically, MI and ME conditions differ in the strategy on how to react to external stimuli. According to Jeannerod's theory (Di Rienzo et al. 2014), MI does not lead to actual motor performance due to the inhibition of motor commands. However, our observation of non-target LRPs in the ME condition but not in MI trials supports the idea that a preselected response strategy influences the patterns of M1 activity for both ME and MI conditions.

We hypothesize that strategy selection could be enabled by a hierarchical structure similar to the "response layer" proposed in the drift-diffusion model (Van Vugt et al. 2014). Frontal areas activated in a stimulus-locked manner could be involved in such a control (Li et al. 2023). We propose a perspective which is different from the prevailing view claiming that response inhibition during MI responses is enacted by a suppression of motor networks. We hypothesize that the parietal areas are subjected to top-down modulations so that they propagate the activity that accumulates during the preparation of imagined responses to non-lateralized networks. This mechanism effectively prevents mapping a stimulus to a real response and explains the absence of lateralized potentials in MI compared with non-target ME trials.

Notably, the presence of this downregulating how-to-respond command could have resulted in non-target LRPs that were incongruent with the stimulus but had a polarity consistent with the target hand. For example, when the right button was the target, non-target LRPs showed the same lateralization as in target trials, regardless of whether they were elicited by left button flashes. Consequently, the polarity of non-target LRPs did not show stimulus–response compatibility (Berlucchi et al. 1977; Holländer et al. 2011), but was consistent with the which-hand-to-respond strategy determined by the prior instruction (also referred to as the precuing effect in Sangals et al. (2002)).

Previous single-unit response experiments in monkeys are useful to tackle our hypothesis. In a classic study, Georgopoulos et al. (1982) observed neuronal discharges in M1 that occurred ~80 ms before the onset of the EMG in the arm muscles and 100–150 ms after a visual cue. Ifft et al. (2012) and Lebedev et al. (1994) reported similar patterns of premovement activity in M1 and S1 elicited by the presentation of visual stimuli instructing movement direction. The timing of these neural patterns was similar to the timing of the LRP we observed here.

RAPs during motor execution and imagery

Numerous studies have investigated the temporal relationship between the late ERP components and movements (Verleger et al. 2006; Saville et al. 2012; Verleger et al. 2014; Berchicci et al. 2016). Consistent with this literature, we observed the development of a contralateral positive motor-related potential after movement onset. This potential was distinct and strong when the epochs traces were aligned on movement onset prior to averaging, and the latency with respect to movement onset was ~200 ms. This cortical potential is known as RAP or movement monitoring potential and has been suggested to originate from precentral regions (Caldara et al. 2004) and somatosensory cortex (Bötzel et al. 1997). The RAP is related to the control of movement execution and somatosensory feedback processing (Bötzel et al. 1997; Berchicci et al. 2016); therefore, the synchrony between movement onset and RAP timing has to be expected.

In our experiments, imagery of pressing a button led to the appearance of positive central-localized potential that had the same latency as the RAP in ME condition. However, the RAP-like MI-related peak was not lateralized. It was suggested that the amplitude of motor-related potentials is proportional to the number of motor units recruited for the performance of a movement (De Morree et al. 2012). As muscle activity was absent during MI, the presence of RAP-like in this condition was somewhat surprising. Several explanations for this effect could be proposed. First, MI-related positivity could have been a late P3 evoked by the target stimulus (Mertens and Polich 1997). However, this potential was absent during the MC trials despite the presence of a mental response to target flash. This result is evident in Fig. 2A, where there is no late positive peak during MC. Secondly, our surface EMG could have been not sufficiently sensitive to detect activity in deeply located muscles and slight (subliminal) muscle twitches (Sosnowska et al. 2021). However, a study using ultrasound imaging to record deep muscles revealed an RAP-like component during MI that developed in the absence of any discernible muscle twitching (Sosnowska et al. 2021). The third possible explanation is offered by the emulation theory (Grush 2004), which suggests the presence of models of the body and environment constructed by the brain to control movements and adapt them to the environment. Sensorimotor efference copies of movements provide expectations of the sensory feedback which are then compared with the afferent inputs during the movement (Greenwald 1970). Such emulation could be run explicitly during MI (Sadato and Naito 2004; Ridderinkhof and Brass 2015), and then RAP-like potential could reflect the activation of cortical areas involved in this emulation. The absence of cortical areas responsible for executing actual motor acts in the cortical substrate of motor emulation results in the non-lateralization of the RAP-like component, similar to the behavior of the sensorimotor ERD, which shows greater lateralization during physical movement compared with MI (Nikulin et al. 2008). Moreover, our analysis revealed that the result of sorting MI epochs based on the estimated RAP-like peak latency shows a remarkable similarity to the pattern observed for real movements: the stimulus-locked negative peak persists until the response-related RAP-like potential, suggesting a comparable "accumulation" process during MI, similar to what is seen before actual motor execution. This process during MI may reflect the preparation and accumulation of activity that precedes the mental sensorimotor response.

β-ERD during MI and ME

We found significant β-ERD in ME and MI trials, but not during MC. For the MI condition, we observed a gradual decrease in β-amplitude for 500–600 ms from target onset. Such β-ERD is consistent with previous MI studies (Pfurtscheller et al. 2008), where it has been considered as a marker of activity in precentral cortical areas (Neuper et al. 2006; Babiloni et al. 2016). Considering the potential connection between the RAP-like component and action emulation processes, as well as the β-ERD induced by imagery reflecting activation of the sensorimotor cortical substrate for movement emulation, exploration is of interest of a potential correlation between these markers. Our analysis of the across-subject correlation between β-ERD amplitude and late positive ERP component revealed strong correlation only for MI but not for ME. This result could be explained by the involvement of reafference-related components during ME, which complicated the relationship between ERD and RAP.

In conclusion, our study provides insights into the role of LRPs during motor preparation and clarifies the accumulation of cortical activity prior to motor execution. The absence of significant lateralized peaks during MI trials challenges the notion that MI has the same mechanism as ME with a difference that a disruption occurs during the final stage of processing. Rather, we suggest that this kind of processing occurs for non-target ME trials, where the visual stimulus initiates early stages of action preparation that could lead to an action but should be halted. We suggest that the differences between the overt and imagined responses observed in this study could be explained in terms of a hierarchical response strategy governing the sensorimotor networks involvement in these behaviors. Our results suggest that activity accumulation starts to occur prior to all types of responses but its lateralization emerges only when response strategy includes the selection of an effector for an overt action.

CRediT taxonomy

Nikolay Syrov: Conceptualization, Data curation, Formal analysis, Investigation, Methodology, Software, Visualization, Writing—original draft; Lev Yakovlev: Data curation, Investigation, Methodology, Writing—original draft; Alexander Kaplan: Conceptualization, Funding acquisition, Supervision, Writing—review & editing; Mikhail Lebedev: Conceptualization, Funding acquisition, Investigation, Project administration, Supervision, Writing—review & editing.

Acknowledgments

The authors acknowledge Alfiia Mustafina for help in preparing the illustrations.

Author contributions

Conceptualization, M.L. and N.S.; Data curation, N.S.; Formal analysis, N.S.; Investigation, N.S. and L.Y.; Methodology, N.S.; Project administration, M.L. and A.K; Resources, M.L. and A.K; Supervision, M.L. and A.K.; Writing original draft, N.S.; Writing—review & editing, L.Y., A.K., and M.L.; All authors have read and agreed to the published version of the manuscript.

Funding

This work was supported by the Russian Science Foundation under grant no. 21-75-30024.

Conflict of interest statement: The authors declare that the research was conducted in the absence of any commercial or financial relationships that could be construed as a potential conflict of interest.

Data availability

The raw data from this study will be made available by the authors upon request without undue restriction.

References

Aflalo T, Zhang C, Revechkis B, Rosario E, Pouratian N, Andersen RA. Implicit mechanisms of intention. *Curr Biol*. 2022:32(9): 2051–2060.

Aksiotis, V., & Ossadtchi, A. Prestimulus beta rhythm influence reaction time during real-time brain-dependent stimuli presentation. In: Kazantsev V, Lobov D, Gordleeva S, Shusharina N. editors. 2022 *Fourth International Conference Neurotechnologies and Neurointerfaces (CNN)*. Kaliningrad: IEEE; 2022. pp. 6–9.

Al E, Stephani T, Engelhardt M, Villringer A, Nikulin VV. Cardiac activity impacts cortical motor excitability. *Res Square*. 2021:2021. https://doi.org/10.21203/rs.3.rs-1023617/v1.

Babiloni C, Del Percio C, Vecchio F, Sebastiano F, Di Gennaro G, Quarato PP, Mirabella G. Alpha, beta and gamma electrocorticographic rhythms in somatosensory, motor, premotor and prefrontal cortical areas differ in movement execution and observation in humans. *Clin Neurophysiol*. 2016:127(1):641–654.

Berchicci M, Spinelli D, Di Russo F. New insights into old waves. Matching stimulus- and response-locked ERPs on the same time-window. *Biol Psychol*. 2016:117(1):202–215.

Berlucchi G, Crea F, Di Stefano M, Tassinari G. Influence of spatial stimulus-response compatibility on reaction time of ipsilateral and contralateral hand to lateralized light stimuli. *J Exp Psychol Hum Percept Perform*. 1977:3(3):505.

Bernstein NA. *O Postrojenii Dvizenij (Über Den Aufbau Der Bewegungen)*. Mozkva: Medgiz; 1947.

Binkofski F, Fink GR, Geyer S, Buccino G, Gruber O, Shah J, Tayler G, Seitz RJ, Zilles K, Freund HJ. Neural activity in the human primary motor cortex areas 4a and 4p is modulated differentially by attention to action. *J Neurophysiol*. 2002:88(1):514–518.

Böcker KBE, Brunia CHM, Cluitmans PJM. A spatio-temporal dipole model of the readiness potential in humans. I. Finger movement. *Electroencephalogr Clin Neurophysiol*. 1994:91(4):275–285.

Bötzel K, Ecker C, Schulze S. Topography and dipole analysis of reafferent electrical brain activity following the Bereitschaftspotential. *Exp Brain Res*. 1997:114(2):352–361.

Caldara R, Deiber MP, Andrey C, Michel CM, Thut G, Hauert CA. Actual and mental motor preparation and execution: a spatiotemporal ERP study. *Exp Brain Res*. 2004:159(3):389–399.

Carrillo-de-la-Pena MT, Lastra-Barreira C, Galdo-Alvarez S. Limb (hand vs. foot) and response conflict have similar effects on event-related potentials (ERPs) recorded during motor imagery and overt execution. *Eur J Neurosci*. 2006:24(2):635–643.

Carrillo-de-la-Peña MT, Galdo-Alvarez S, Lastra-Barreira C. Equivalent is not equal: primary motor cortex (MI) activation during motor imagery and execution of sequential movements. *Brain Res*. 2008:1226:134–143.

Coles MG. Modern mind-brain reading: psychophysiology, physiology, and cognition. *Psychophysiology*. 1989:26(3):251–269.

De Morree HM, Klein C, Marcora SM. Perception of effort reflects central motor command during movement execution. *Psychophysiology*. 2012:49(9):1242–1253.

Deecke L, Grözinger B, Kornhuber HH. Voluntary finger movement in man: cerebral potentials and theory. *Biol Cybern*. 1976:23(2): 99–119.

Di Rienzo F, Guillot A, Daligault S, Delpuech C, Rode G, Collet C. Motor inhibition during motor imagery: a MEG study with a quadriplegic patient. *Neurocase*. 2014:20(5):524–539.

Fadiga L, Buccino G, Craighero L, Fogassi L, Gallese V, Pavesi G. Corticospinal excitability is specifically modulated by motor imagery: a magnetic stimulation study. *Neuropsychologia*. 1998:37(2): 147–158.

Fairhall SL, Kirk IJ, Hamm JP. Volition and the idle cortex: beta oscillatory activity preceding planned and spontaneous movement. *Conscious Cogn*. 2007:16(2):221–228.

Falkenstein M, Yordanova J, Kolev V. Effects of aging on slowing of motor-response generation. *Int J Psychophysiol*. 2006:59(1): 22–29.

Gabbard C, Cordova A, Lee S. A question of intention in motor imagery. *Conscious Cogn*. 2009:18(1):300–305.

Galdo-Alvarez S, Bonilla FM, González-Villar AJ, Carrillo-De-la-Pena MT. Functional equivalence of imagined vs. real performance of an inhibitory task: an EEG/ERP study. *Front Hum Neurosci*. 2016:10:467.

Ganin I, Kaplan A. Study of the human brain potentials variability effects in P300 based brain–computer interface. *Bull Russ State Medical Univ*. 2022:3(1):75–82.

Georgopoulos AP, Kalaska JF, Caminiti R, Massey JT. On the relations between the direction of two-dimensional arm movements and cell discharge in primate motor cortex. *J Neurosci*. 1982:2(11): 1527–1537.

Gherman S, Markowitz N, Tostaeva G, Espinal E, Mehta AD, O’Connell RG, Bickel S. Intracranial electroencephalography reveals effector-independent evidence accumulation dynamics in multiple human brain regions. *bioRxiv*. 2023:2023–2004.

Glover S, Dixon P. Context and vision effects on real and imagined actions: support for the common representation hypothesis of motor imagery. *J Exp Psychol Hum Percept Perform*. 2013:39(5):1352.

Glover S, Bibby E, Tuomi E. Executive functions in motor imagery: support for the motor-cognitive model over the functional equivalence model. *Exp Brain Res*. 2020:238(4):931–944.

Gratton G, Kramer AF, Coles MG, Donchin E. Simulation studies of latency measures of components of the event-related brain potential. *Psychophysiology*. 1989:26(2):233–248.

Greenwald AG. Sensory feedback mechanisms in performance control: with special reference to the ideo-motor mechanism. *Psychol Rev*. 1970:77(2):73.

Grosprêtre S, Ruffino C, Lebon F. Motor imagery and cortico-spinal excitability: a review. *Eur J Sport Sci*. 2016:16(3):317–324.

Grush R. The emulation theory of representation: motor control, imagery, and perception. *Behav Brain Sci*. 2004:27(3):377–396.

Guillot A, Collet C, Nguyen VA, Malouin F, Richards C, Doyon J. Brain activity during visual versus kinesthetic imagery: an fMRI study. *Hum Brain Mapp*. 2009:30(7):2157–2172.

Guthrie MD, Gilbert DL, Huddleston DA, Pedapati EV, Horn PS, Mostofsky SH, Wu SW. Online transcranial magnetic stimulation protocol for measuring cortical physiology associated with response inhibition. *J Vis Exp*. 2018:132:e56789.

Hackley SA, Valle-Inclan F. Automatic alerting does not speed late motoric processes in a reaction-time task. *Nature*. 1998:391(6669): 786–788.

Hanes DP, Schall JD. Neural control of voluntary movement initiation. *Science*. 1996:274(5286):427–430.

Hanks TD, Kopec CD, Brunton BW, Duan CA, Erlich JC, Brody CD. Distinct relationships of parietal and prefrontal cortices to evidence accumulation. *Nature*. 2015:520(7546):220–223.

Hohlefeld FU, Nikulin VV, Curio G. Visual stimuli evoke rapid activation (120 ms) of sensorimotor cortex for overt but not for covert movements. *Brain Res*. 2011:1368:185–195.

Holländer A, Jung C, Prinz W. Covert motor activity on NoGo trials in a task sharing paradigm: evidence from the lateralized readiness potential. *Exp Brain Res*. 2011:211(3):345–356.

Ifft PJ, Lebedev MA, Nicolelis MA. Reprogramming movements: extraction of motor intentions from cortical ensemble activity when movement goals change. *Front Neuroeng*. 2012:5:16.

Jeannerod M. Mechanisms of visuomotor coordination: a study in normal and brain-damaged subjects. *Neuropsychologia*. 1986:24(1): 41–78.

Jeannerod M. The representing brain: Neural correlates of motor intention and imagery. *Behavioral and Brain sciences*. 1994:17(2):187–202.

Jeannerod M. Neural simulation of action: a unifying mechanism for motor cognition. *NeuroImage*. 2001:14(1):S103–S109.

Jennings JR, van der Molen MW. Preparation for speeded action as a psychophysiological concept. *Psychol Bull*. 2005:131(3):434.

Ko YT, Cheng SK, Juan CH. Voluntarily-generated unimanual preparation is associated with stopping success: evidence from LRP and lateralized mu ERD before the stop signal. *Psychol Res*. 2015:79: 249–258.

Kunzendorf S, Klotzsche F, Akbal M, Villringer A, Ohl S, Gaebler M. Active information sampling varies across the cardiac cycle. *Psychophysiology*. 2019:56(5):e13322.

Lebedev MA, Denton JM, Nelson RJ. Vibration-entrained and premovement activity in monkey primary somatosensory cortex. *J Neurophysiol*. 1994:72(4):1654–1673.

Li G, Jiang S, Meng J, Wu Z, Jiang H, Fan Z, Zhu X. Spatio-temporal evolution of human neural activity during visually cued hand movements. *Cereb Cortex*. 2023:33(17):9764–9777.

Logan GD, Cowan WB. On the ability to inhibit thought and action: a theory of an act of control. *Psychol Rev*. 1984:91(3):295.

Luck SJ, Kappenman ES, Fuller RL, Robinson B, Summerfelt A, Gold JM. Impaired response selection in schizophrenia: evidence from the P3 wave and the lateralized readiness potential. *Psychophysiology*. 2009:46(4):776–786.

Makeig S, Onton J. ERP features and EEG dynamics: an ICA perspective. In: Luck S, Kappenman E. editors. *Oxford handbook of event-related potential components*. New York: Oxford University Press; 2012. pp. 51–88.

McFarland DJ, McCane LM, David SV, Wolpaw JR. Spatial filter selection for EEG-based communication. *Electroencephalogr Clin Neurophysiol*. 1997:103(3):386–394.

Mehler DM, Williams AN, Krause F, Lührs M, Wise RG, Turner DL, Whittaker JR. The BOLD response in primary motor cortex and supplementary motor area during kinesthetic motor imagery based graded fMRI neurofeedback. *NeuroImage*. 2019:184(1): 36–44.

Mertens R, Polich J. P300 from a single-stimulus paradigm: passive versus active tasks and stimulus modality. *Electroencephalogr Clin Neurophysiol*. 1997:104(6):488–497.

Misirlisoy E, Haggard P. Veto and vacillation: a neural precursor of the decision to withhold action. *J Cogn Neurosci*. 2014:26(2):296–304.

Murakami M, Vicente MI, Costa GM, Mainen ZF. Neural antecedents of self-initiated actions in secondary motor cortex. *Nat Neurosci*. 2014:17(11):1574–1582.

Murakami M, Shteingart H, Loewenstein Y, Mainen ZF. Distinct sources of deterministic and stochastic components of action timing decisions in rodent frontal cortex. *Neuron*. 2017:94(4): 908–919.

Neafsey EJ. Conscious intention and human action: review of the rise and fall of the readiness potential and Libet's clock. *Conscious Cogn*. 2021:94:103171.

Neuper C, Wörtz M, Pfurtscheller G. ERD/ERS patterns reflecting sensorimotor activation and deactivation. *Prog Brain Res*. 2006:159: 211–222.

Nikulin VV, Hohlefeld FU, Jacobs AM, Curio G. Quasi-movements: a novel motor–cognitive phenomenon. *Neuropsychologia*. 2008:46(2): 727–742.

O'Shea H, Moran A. Does motor simulation theory explain the cognitive mechanisms underlying motor imagery? A critical review. *Front Hum Neurosci*. 2017:11:72.

Paluch K, Jurewicz K, Wróbel A. Beyond difference in reaction time: understanding neuronal activity during the preparatory period of the decision process. *J Cogn Neurosci*. 2021:33(2):263–278.

Pfurtscheller G, Neuper C. Motor imagery activates primary sensorimotor area in humans. *Neuroscience letters*. 1997:239(2–3): 65–68.

Pfurtscheller G. Spatiotemporal ERD/ERS patterns during voluntary movement and motor imagery. *Suppl Clin Neurophysiol*. 2000:53: 196–198.

Pfurtscheller G, Graimann B, Huggins JE, Levine SP, Schuh LA. Spatiotemporal patterns of beta desynchronization and gamma synchronization in corticographic data during self-paced movement. *Clin Neurophysiol*. 2003:114(7):1226–1236.

Pfurtscheller G, Scherer R, Müller-Putz GR, Lopes da Silva FH. Short-lived brain state after cued motor imagery in naive subjects. *Eur J Neurosci*. 2008:28(7):1419–1426.

Picton TW, Bentin S, Berg P, Donchin E, Hillyard SA, Johnson R, Taylor MJ. Guidelines for using human event-related potentials to study cognition: recording standards and publication criteria. *Psychophysiology*. 2000:37(2):127–152.

Poli R, Cinel C, Citi L, Sepulveda F. Reaction-time binning: a simple method for increasing the resolving power of ERP averages. *Psychophysiology*. 2010:47(3):467–485.

Rahman M, Karwowski W, Fafrowicz M, Hancock PA. Neuroergonomics applications of electroencephalography in physical activities: a systematic review. *Front Hum Neurosci*. 2019:13:182.

Ridderinkhof KR, Brass M. How kinesthetic motor imagery works: a predictive-processing theory of visualization in sports and motor expertise. *J Physiol*. 2015:109(1–3):53–63.

Rodriguez M, Llanos C, Sabate M. The kinematics of motor imagery: comparing the dynamics of real and virtual movements. *Neuropsychologia*. 2009:47(2):489–496.

Rogge J, Jocham G, Ullsperger M. Motor cortical signals reflecting decision making and action preparation. *NeuroImage*. 2022:263:119667.

Sadato N, Naito E. Emulation of kinesthesia during motor imagery. *Behav Brain Sci*. 2004:27(3):412–413.

Sangals J, Sommer W, Leuthold H. Influences of presentation mode and time pressure on the utilisation of advance information in response preparation. *Acta Psychol*. 2002:109(1):1–24.

Savaki HE, Raos V. Action perception and motor imagery: mental practice of action. *Prog Neurobiol*. 2019:175:107–125.

Saville CW, Shikhare S, Iyengar S, Daley D, Intriligator J, Boehm SG, Klein C. Is reaction time variability consistent across sensory modalities? Insights from latent variable analysis of single-trial P3b latencies. *Biol Psychol*. 2012:91(2):275–282.

Saville CW, Feige B, Kluckert C, Bender S, Biscaldi M, Berger A, Klein C. Increased reaction time variability in attention-deficit hyperactivity disorder as a response-related phenomenon: evidence from single-trial event-related potentials. *J Child Psychol Psychiatry*. 2015:56(7):801–813.

Schmitz J, Packheiser J, Birnkraut T, Hinz NA, Friedrich P, Güntürkün O, Ocklenburg S. The neurophysiological correlates of handedness: insights from the lateralized readiness potential. *Behav Brain Res*. 2019:364:114–122.

Schnitzler A, Salenius S, Salmelin R, Jousmäki V, Hari R. Involvement of primary motor cortex in motor imagery: a neuromagnetic study. *NeuroImage*. 1997:6(3):201–208.

Schultze-Kraft M, Birman D, Rusconi M, Allefeld C, Görgen K, Dähne S, Haynes JD. The point of no return in vetoing self-initiated movements. *Proc Natl Acad Sci*. 2016:113(4):1080–1085.

Sosnowska A, Gollee H, Vučković A. MRCP as a biomarker of motor action with varying degree of central and peripheral contribution as defined by ultrasound imaging. *J Neurophysiol*. 2021:126(1): 249–263.

Stinear CM, Byblow WD, Steyvers M, Levin O, Swinnen SP. Kinesthetic, but not visual, motor imagery modulates corticomotor excitability. *Exp Brain Res*. 2006:168:157–164.

Stippich C, Ochmann H, Sartor K. Somatotopic mapping of the human primary sensorimotor cortex during motor imagery and motor execution by functional magnetic resonance imaging. *Neurosci Lett*. 2002:331(1):50–54.

Syrov N, Yakovlev L, Nikolaeva V, Kaplan A, Lebedev M. Mental strategies in a P300-BCI: Visuomotor transformation is an option. *Diagnostics*. 2022:12(11):2607.

Trevena JA, Miller J. Cortical movement preparation before and after a conscious decision to move. *Conscious Cogn*. 2002:11(2): 162–190.

Van Vugt MK, Simen P, Nystrom L, Holmes P, Cohen JD. Lateralized readiness potentials reveal properties of a neural mechanism for implementing a decision threshold. *PLoS One*. 2014:9(3):e90943.

Vaughan Jr. The relationship of brain activity to scalp recordings of event-related potentials. In: Donchin IE, Lindsley DB, editors. *Average evoked potentials. Methods, results and evaluations*. Washington, DC: National Aeronautics and Space Administration; 1969. pp. 45–75.

Verleger R, Paehge T, Kolev V, Yordanova J, Jaśkowski P. On the relation of movement-related potentials to the go/no-go effect on P3. *Biol Psychol*. 2006:73(3):298–313.

Verleger R, Baur N, Metzner MF, Śmigasiewicz K. The hard oddball: effects of difficult response selection on stimulus-related P 3 and on response-related negative potentials. *Psychophysiology*. 2014:51(11):1089–1100.

Yashin AS, Shishkin SL, Vasilyev AN. Is there a continuum of agentive awareness across physical and mental actions? The case of quasi-movements. *Conscious Cogn*. 2023:112:103531.

Yousry TA, Schmid UD, Alkadhi H, Schmidt D, Peraud A, Buettner A, Winkler P. Localization of the motor hand area to a knob on the precentral gyrus. A new landmark. *Brain J Neurol*. 1997:120(1): 141–157.